

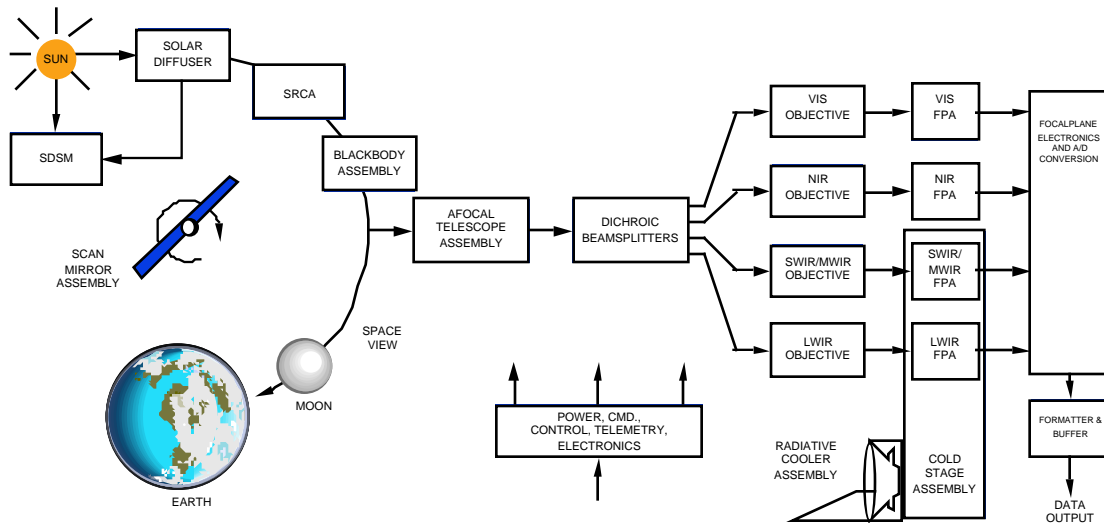
# PRE-LAUNCH ALGORITHM AND DATA FORMAT FOR THE LEVEL 1 CALIBRATION PRODUCTS FOR THE EOS AM-1 MODERATE RESOLUTION IMAGING SPECTRORADIOMETER (MODIS)

B. Guenther , Gerald D. Godden , Xiaoxiong Xiong , Edward J. Knight , Harry Montgomery , M. M. Hopkins , Mohammad G. Khayat and Zhidong Hao

## ABSTRACT

The MODIS radiometric calibration product (Level 1B) is described for the emissive and the reflective solar bands. Specific information on the sensor design characteristics are identified to assist in the understanding of how the calibration algorithm product is developed. The reflected solar band products of radiance and reflectance factor both are described. The product file format is summarized and the MCST Homepage location for the current file format is listed.

## MODIS DESIGN FROM PHOTONS TO DATA



Guenther and Montgomery are employed by NASA's Goddard Space Flight Center, Greenbelt, MD 20771.

Godden is employed by Physics Application, Inc, Vienna, VA

Xiong is employed by Science Systems and Applications, Inc, Lanham, MD 20706

Knight and Khayat are employed by Research and Data Systems Corporation, Greenbelt, MD 20770

Hopkins and Hao are employed by General Sciences Corporation, Laurel, MD 20707

Corresponding Author: B. Guenther, Mail Code 920.1, GSFC, Greenbelt, MD 20771; telephone (301)286-5205; fax (301)286-0373; email [guenther@ltpmail.gsfc.nasa.gov](mailto:guenther@ltpmail.gsfc.nasa.gov)

## 1.0 Introduction

The calibrated, Earth-located data products for MODIS are produced in Level 1 processes. The development of the science products begin with these Level 1 products. This paper describes the calibration algorithms used to produce the MODIS Level 1B (L1B) product. The characteristics of geometric registration and spectral characterization are not handled directly in this paper. The primary aspects of the MODIS sensor are described in Barnes, et. al., 1998 in this issue. Two overview descriptions of MODIS science products also are included in this issue, one by Esaias, et al., 1998 and one by Justice, et. al., 1998. The process to provide the Earth location (geometric registration) of the MODIS data set is described elsewhere in this series of papers, Masuoka, et. al., 1998. The calibration algorithms which are used for the Level 1B product are described. The work developing the calibration algorithm for the MODIS Science Team is performed at NASA's Goddard Space Flight Center by the MODIS Characterization Support Team (MCST).

Sensor design and characteristics necessary to understand the Level 1B product are reviewed in the Section Instrument Background. The emissive infrared algorithms are described in the next Section. The pre-launch calibration algorithm, the on-orbit radiometric algorithm, and the on-orbit maneuver to determine the scan mirror response vs scan angle are reviewed separately. The reflected solar bands algorithm, including subsections on the radiance and the reflectance factor products are covered in the following Section. The Level 1B data product attributes such as file, format and uncertainty index are reviewed in Section 5.0. Section 6.0 provides the summary and final comments.

The primary techniques for tracking the sensor radiometric performance on-orbit as required for these calibration algorithms is identified with each algorithm.

## 2.0 Instrument Background

A schematic of the internal MODIS scan cavity is provided in Figure 1. The MODIS design incorporates several on-board calibration (OBC) targets and each are valuable for some aspects of the calibration algorithm design. The Figure shows that the scan mirror can access internal OBCs of the solar diffuser (SD), the spectroradiometric calibration assembly (SRCA), the blackbody (BB) and cold space view (SV). Each of these OBC targets are accessed by the scan mirror on each mirror rotation, and they are seen within a rotation (frame) before the Earth view. The location within a frame is identified as the Principal Scan Angle. Figure 2 shows the orientation of each OBC, the location of the Earth view around the scan as well as the location of the principal on-the-ground laboratory calibration sources. This Figure also indicates how the Principal Scan Angle maps for the angle of incidence on the scan mirror. The scan mirror is double sided and both sides are used for the MODIS observations.

Light from an individual target or view reflects from the scan mirror and enters into the telescope. The spectral separation for MODIS is accomplished with a set of dichroic beamsplitters, and individual interference filters. Additional spectral shaping is provided by mirrors, filter masks, anti-reflectance coatings on the optics, and intermediate filters located on the LWIR and SWIR/MWIR paths. MODIS bands are separated into four focal plan assemblies, with bands with center wavelengths between 0.42 to 0.55  $\mu\text{m}$  on the VIS, with 0.64 to 0.94  $\mu\text{m}$  on the NIR, with 1.2 to 4.5  $\mu\text{m}$  on the SWIR/MWIR and 6.5 to 14.2  $\mu\text{m}$  on the LWIR focal planes. Information on the spectral bandpasses for MODIS is included in Barnes, et. al., 1998, and the definitive relative spectral responses available through MCST Homepage on the World Wide Web at <http://ftpwww.gsfc.nasa.gov/MODIS/MCST/Home.html>, under the button "Individual Bands Data."

The scan mirror has a “Denton” silver coating, selected to support measurements below 0.5  $\mu\text{m}$  to have low polarization sensitivity throughout the reflected solar bands. This coating does have a variation in reflectance as a function of angle of incidence on the mirror in the emissive infrared due to different reflectance for the s and p polarization of the incident light beam.

The OBC BB is designed to “float” at the sensor cavity temperature. The V-grooved design has a high emissivity (0.994) in the direction which MODIS views it. It is fitted with 12 temperature sensors behind the emissive surface, and is capable of being heated to 315K on orbit. The expected operating temperature of the OBC BB initially on-orbit is about 268K.

The SD is a Spectralon™ reflecting surface. Typical reflectance for this target is provided in Figure 3, from the manufacturer specifications, Labsphere, 1996. Note the particular flat response across all the MODIS reflected solar bands, except for the structure at 2.1  $\mu\text{m}$ . The Solar Diffuser Stability Monitor (SDSM) is a subsystem which measures the incident sunlight and the sunlight reflected off the SD as a ratio. This subsystem will provide knowledge on the effective BRDF of the SD for each SD-sun measurement. There are nine silicon photodetectors for the SDSM, housed in a Spectralon™ coated miniature integrating sphere.

The MODIS fore-optics have been kept clean during manufacturer and testing, as well as during the spacecraft integration of the sensor. Nevertheless, we expect to have a cleanliness level at launch of about 300, with an anticipated cleanliness level rising quickly to about 350-400 on orbit due to dust and possible mirror pitting. These real optics will demonstrate a light scattering which will make it difficult to work in the reflected solar portion of the MODIS spectrum near cloud edges and other areas of high spatial contrast.

MCST intends to publish an index which relates to the contrast in each scene as it effects individual pixels on orbit, to assist the data users in distinguishing measurements which are more or less impacted by this scattering feature. This scattering index is not described in this paper but will be described with the Level 1B (L1B) file format. The complete file format for the L1B is best obtained through the MCST Homepage on the World Wide Web, under the button “software.” The scattering is not expected to be important in the emissive infrared bands for MODIS.

The SRCA is used for on-orbit geometric registration knowledge and control, spectral bandpass knowledge for the reflected solar bands, and radiometric stability verification of the reflected solar bands. The SRCA characteristics which is needed in the context of this paper is the feature that it can operate on-orbit for an extended period of time putting low light levels onto the VIS/NIR/SWIR bands. This characteristic is being used to verify that the pre-launch temperature characterization of MODIS is adequate for tracking the MODIS changes within an orbit, due to changes in the thermal behavior.

The geometric registration features of the SRCA are useful for characteristics described in Masuoka, et. al., 1998, and the spectral characteristics are needed for actual sensor spectral characteristics, and will be used in the spectral characterization identified on the MCST Homepage.

### **3.0 MODIS Thermal Emissive Bands Radiometric Calibration Algorithm**

The NASA Goddard Space Flight Center MODIS Calibration Support Team (MCST) has pursued two independent calibration methodologies for the MODIS thermal bands. The first method is based on the traditional technique of fitting the instrument output digital numbers (DNs) versus radiance [Watts/(m<sup>2</sup>\*sr\*micrometer)] distribution to a quadratic polynomial expression, and is similar in form to the algorithm suggested by Young, 1997. This is referred to as the L vs DN algorithm. The second method is based on a somewhat more physical approach of converting the output DN's to detector output voltages, incorporating the telemetered DC restore voltage offsets, and then fitting these results to a second order equation that applies a local curvature as a function of the signal level. This is referred to as the V vs L algorithm and is described by Knowles, et al, 1996. This paper presents an overview of the first method, which is planned to be the baseline algorithm at launch. Investigation of the more complex V vs L algorithm performance and comparison with the L vs DN algorithm is a subject of continuing research, and is not presented here.

The MODIS thermal emissive bands (Bands 20-25, and 27-36) covering the wavelength region from 3.75 to 14.24 μm, and consisting of 10 channels per band, are radiometrically calibrated using a precision Blackbody Calibration Source (BCS) which is contained within the Thermal Vacuum chamber with the MODIS during calibration. The BCS is of the "buried-first bounce" type design and is expected to have an emissivity of 0.9995. It is located at -45 degree scan angle with respect to the MODIS nadir viewing scan position in the 110 degree Earth view scan angle range. This translates into a low scan angle Angle-of-Incidence (AOI) (15.5 degrees) on the scan mirror to minimize reflectance variation effects. The on-board calibrator blackbody (OBC BB) and Space View Port are viewed once per scan mirror rotation by each side of the scan mirror. During Thermal Vacuum calibration the Space View Port is covered with a cryogenically cooled Space View Source (SVS) to simulate the on-orbit view of cold space.

The silver coated scan mirror exhibits a significant variation of average reflectance as a function of wavelength, Cafferty, 1995 and MacDonald, 1997. In addition to the wavelength dependent reflectivity for the scan mirror, the AOI locations of the BCS, OBC BB and the SVS are critical factors which must be incorporated into the algorithm. The location of these sources along a scan are depicted in Figure 2.

The primary calibration in the laboratory is based on the laboratory BCS. The BCS calibration is applied to the OBC BB, and the on-orbit calibration is maintained with the OBC BB and SV combination.

### 3.1 Pre-launch Radiometric Calibration Algorithm

The MODIS is a conventional differencing radiometer. Instrument background radiation effects are removed by subtracting the cold space view signal from the earth view signal on a scan-by-scan basis. During Thermal Vacuum calibration the spectral radiance from the Blackbody Calibration Source (BCS), after reflection from the scan mirror is given by:

$$L_{BCS\_PATH} = \frac{sm}{BCS} BCS L(T_{BCS}) + (1 - \frac{sm}{BCS}) L(T_{sm}) + L_{BKG} \quad (1)$$

where  $\frac{sm}{BCS}$  is the scan mirror reflectivity at the AOI for the BCS,  $BCS$  represents the BCS emissivity,  $L(T_{BCS})$  is the radiance calculated from the Planck equation at the BCS temperature  $T_{BCS}$ ,  $L(T_{sm})$  is the radiance calculated from the Planck equation at scan mirror temperature  $T_{sm}$ , and  $L_{BKG}$  is the instrument background radiance exclusive of

the scan mirror emission. The second term of this equation represents the emission from the scan mirror. This term is separated out from the total instrument background to explicitly capture its scan angle and temperature dependence.

Similarly, when MODIS views the Space View Source, the spectral radiance after the scan mirror is given by:

$$L_{SVS\_PATH} = (1 - \frac{sm}{SVS})L(T_{sm}) + L_{BKG} \quad (2)$$

To remove the variable instrument background effect, the Space View Source term is subtracted from the input signal, and thus, the spectral radiance difference is:

$$L_{BCS} = L_{BCS\_PATH} - L_{SVS\_PATH} = \frac{sm}{BCS} BCS L(T_{BCS}) + (\frac{sm}{SVS} - \frac{sm}{BCS})L(T_{sm}) \quad (3)$$

For a specific MODIS thermal emissive band (B), the band averaged radiance difference due the BCS path and the SVS path is:

$$L_{BCS}(B) = \overline{\frac{sm}{BCS} BCS L(T_{BCS})} + \overline{(\frac{sm}{SVS} - \frac{sm}{BCS})L(T_{sm})} \quad (4)$$

where

$$\overline{\frac{sm}{BCS} BCS L(T_{BCS})} = \frac{\overline{\frac{sm}{BCS}(\lambda) BCS(\lambda) L(T_{BCS}, \lambda) RSR(B, \lambda) d}}{RSR(B, \lambda) d} \quad (5)$$

and  $RSR(B, \lambda)$  represents the wavelength dependent Relative Spectral Response (normalized to unity at peak) for the  $B^{th}$  band, and a similar expression for the band averaging applies to the second term on the RHS of Eqn. 4. N.B., through out this discussion, the channel number indices are suppressed for clarity.

The band averaged radiance difference  $L_{BCS}(B)$  is a function of  $DN_{BCS} - DN_{SVS}$ . Let

$$dn_{BCS} = \frac{1}{N_{scans}} \sum_{n=1}^{N_{scans}} \frac{1}{M_{BCS}} \sum_{m=1}^{M_{BCS}} DN_{BCS} - \frac{1}{M_{SVS}} \sum_{m=1}^{M_{SVS}} DN_{SVS} \quad (6)$$

where  $M_{BCS}$ ,  $M_{SVS}$  and  $N_{scans}$ , are appropriately chosen averaging span constants.

On the basis of experience with similar instruments, and observed temperature dependencies, we postulate a temperature dependent second order nonlinear behavior for  $L_{BCS}(B, T_{instr})$

$$L_{BCS}(B, T_{instr}) = a_0^{BCS}(B, T_{instr}) + a_1^{BCS}(B, T_{instr}) dn_{BCS} + a_2^{BCS}(B, T_{instr}) (dn_{BCS})^2 \quad (7)$$

Then,

$$\frac{sm}{BCS}L(T_{BCS}) + \left( \frac{sm}{SVS} - \frac{sm}{BCS} \right) L(T_{sm}) = a_0^{BCS}(B, T_{instr}) + a_1^{BCS}(B, T_{instr}) dn_{BCS} + a_2^{BCS}(B, T_{instr}) (dn_{BCS})^2 \quad (8)$$

The BCS calibration coefficients  $a_0^{BCS}(B, T_{instr})$ ,  $a_1^{BCS}(B, T_{instr})$ , and  $a_2^{BCS}(B, T_{instr})$  are then determined by least-squares fitting to the corresponding data. It should be noted that in principle, the constant term  $a_0^{BCS}$  should be zero since Eqn (7) uses  $dn$ 's which already accommodate the MODIS response to the zero radiance scene of cold space. This term is viewed as part of the least squares fitting process. Thus  $a_0^{BCS}$  can be expected to take on small non-zero values. The contribution from the nonlinear response term  $a_2^{BCS}(B, T_{instr})$  is expected to be very small compared to the linear response term. Apart from its temperature dependent behavior,  $a_2^{BCS}(B, T_{instr})$  will be fixed for the on-orbit operation.

### 3.2 On-Orbit Radiometric Algorithm

When MODIS views the on-board blackbody (OBC BB), the spectral radiance after the scan mirror includes the OBC BB emitted radiance reflected by the scan mirror, the scan mirror emittance, the scan cavity emittance reflected by the OBC BB and then in turn by the scan mirror, and the remaining instrument background radiance. Thus

$$L_{BB\_PATH} = BB L(T_{BB}) \frac{sm}{BB} + \left( 1 - \frac{sm}{BB} \right) L(T_{sm}) + L_{cav} L(T_{cav}) \left( 1 - \frac{sm}{BB} \right) \frac{sm}{BB} + L_{BKG} \quad (9)$$

where  $\epsilon_{BB}$  is the OBC BB emissivity,  $(1 - \epsilon_{BB})$  is the reflectivity of the OBC BB, and  $\epsilon_{cav}$  represents the MODIS scan cavity effective emissivity which must account for the Earth and Space View apertures.

From Eqn .9 and 2, the spectral radiance difference attributed to the OBC BB path and the Space View path is given by:

$$\begin{aligned} L_{BB} &= L_{BB\_PATH} - L_{SV\_PATH} \\ &= \epsilon_{BB}^{sm} L(T_{BB}) + (\epsilon_{SV}^{sm} - \epsilon_{BB}^{sm}) L(T_{sm}) \\ &\quad + (1 - \epsilon_{BB}) \epsilon_{cav} \epsilon_{BB}^{sm} L(T_{cav}) \end{aligned} \quad (10)$$

For a specific MODIS band, the band averaged radiance difference between the OBC BB path and the Space View path is given by:

$$\begin{aligned} L_{BB}(B) &= \overline{\epsilon_{BB}^{sm} L(T_{BB})} + \overline{(\epsilon_{SV}^{sm} - \epsilon_{BB}^{sm}) L(T_{sm})} \\ &\quad + (1 - \epsilon_{BB}) \epsilon_{cav} \overline{\epsilon_{BB}^{sm} L(T_{cav})} \end{aligned} \quad (11)$$

where

$$\overline{\epsilon_{BB}^{sm} L(T_{BB})} = \frac{\int \epsilon_{BB}^{sm}(B) L(T_{BB}) RSR(B, \lambda) d\lambda}{\int RSR(B, \lambda) d\lambda} \quad (12)$$

and similarly for the second and third terms on the RHS of Eqn. 11.

The earth view sector digital data is determined using the on-orbit calibration coefficients determined using the OBC BB and the Space View, and the pre-launch second order calibration coefficients determined from the Thermal Vacuum BCS data sets. Equation 13 describes these coefficients:

$$L_{BB}(B, T_{instr}) = a_0^{BCS}(B, T_{instr}) + b_1^{BB}(B, T_{instr}) \cdot dn_{BCS} + a_2^{BCS}(B, T_{instr}) \cdot (dn_{BCS})^2 \quad (13)$$

where  $b_1^{BB}(B, T_{instr})$  are determined on a scan-by-scan basis, described below; and the residual offset coefficient  $a_0^{BCS}(B, T_{instr})$  and second order coefficients,  $a_2^{BCS}(B, T_{instr})$  are determined as described above in Eqn. 8.

The linear portion of the total instrument response on a scan-by-scan basis is:

$$b_1^{BB}(B) = \frac{L_{BB}(B) - a_0^{BCS}(B) - a_2^{BCS}(B) \cdot (dn_{BB})^2}{dn_{BB}} \quad (14)$$

where  $L_{BB}(B)$  is given by Eqn. 11, and

$$dn_{BB} = \frac{1}{M_{BB}} \sum_{i=1}^{M_{BB}} DN_{BB} - \frac{1}{M_{SV}} \sum_{i=1}^{M_{SV}} DN_{SV} \quad (15)$$

To achieve slowly varying behavior the linear response term is averaged over  $N_{scans}$

$$\overline{b_1^{BB}(B)} = \frac{1}{N_{scans}} \sum_{j=1}^{N_{scans}} dn_{BB} \quad (16)$$

The MODIS scan mirror takes 2.954 seconds to complete a rotation. During each scan a new measurement of the linear response (gain) is determined, according to Eqn. 14. The drift of the gain from scan to scan is expected to be very small. This slowly varying behavior is considered by averaging the linear response term over  $N_{scans}$  as shown in Eqn. 16.

The OBC BB will be cycled to 315K and allowed to return to the sensor thermal ambient temperature on an approximately bi-weekly basis. This cycle will allow for a determination of  $b_1^{BB-elev}(B)$ . Comparison of  $b_1^{BB-elev}(B)$  with  $b_1^{BB}(B, T_{instr.})$  will verify the continued stability of on-orbit operation of  $a_0^{BCS}$  and  $a_2^{BCS}$ . Vicarious calibration measurements obtained during the Validation phase of the MODIS also will be used to verify the stability on-orbit operation of  $a_0^{BCS}$  and  $a_2^{BCS}$  and the performance of the OBC BB.

There is a small time difference between when the gain is calculated and when the Earth view data is collected. During this time interval the instrument background may be expected to drift a small relative amount due to 1/f noise. In a manner analogous to that suggested by Knowles, et al., 1996, a portion of this drift can be reduced by linear interpolation between successive scans.

Using the average gain (i.e. the linear response) the difference,  $b_i^{BB}$ , between the  $i^{th}$  measurement, and the average of many measurements of the OBC blackbody is given by:

$$\overline{dn_{BB,i}^{BB}} = dn_{BB,i} - \overline{dn_{BB,i}} = dn_{BB,i} - \frac{L_{BB,i}^{Linear}(B) - a_0^{BCS}(B)}{\overline{b_{1,i}^{BB}}} \quad (17)$$

Similarly for the scan i+1:

$$\overline{dn_{BB,i+1}^{BB}} = dn_{BB,i+1} - \overline{dn_{BB,i+1}} = dn_{BB,i+1} - \frac{L_{BB,i+1}^{Linear}(B) - a_0^{BCS}(B)}{\overline{b_{1,i+1}^{BB}}} \quad (18)$$

The instantaneous correction to  $dn_{EV}$  is given by adding the linearly interpolated amount, according to:

$$dn_{EV}(t) = dn_{ev}(t) + \frac{\overline{dn_{BB,i+1}^{BB}} - \overline{dn_{BB,i}^{BB}}}{2.954} t + \frac{\overline{dn_{BB,i}^{BB}}}{i} \quad (19)$$

where the time,  $t$ , is measured from the center of the  $i^{th}$  scan measurement of the OBC blackbody.

Generalizing Eq. 3, the radiance difference attributed to the Earth View path and the Space View path (after reflection by the scan mirror) is given by:

$$L_{EV} = L_{EV\_PATH} - L_{SVS\_PATH} = \overline{\rho_{EV}^{sm}} L_{EV} + (\overline{\rho_{SV}^{sm}} - \overline{\rho_{EV}^{sm}}) L(T_{sm}) \quad (20)$$

and similarly from Eq. 8:

$$\overline{\rho_{EV}^{sm}} L_{EV} + (\overline{\rho_{SV}^{sm}} - \overline{\rho_{EV}^{sm}}) L(T) = a_0^{BCS} + \overline{b_1^{BB}} \cdot dn_{EV} + a_2^{BCS} \cdot (dn_{EV})^2 \quad (21)$$

where the overstrike bar over the terms on the LHS of Eq. 19 indicate the appropriate RSR averaging similar to Eqn 5 and 12.

Solving Eq. 21 for the band averaged radiance from the Earth View, before the scan mirror reflection, representing the desired “at aperture” radiance,  $\overline{L_{EV}}$  yields:

$$\overline{L_{EV}(B)} = \frac{\frac{1}{\overline{\rho_{EV}^{sm}(\lambda)}} \cdot \left[ a_0^{BCS} + \overline{b_1^{BB}} \cdot dn_{EV} + a_2^{BCS} \cdot (dn_{EV}) - \left\{ \overline{\rho_{SV}^{sm}(\lambda)} - \overline{\rho_{EV}^{sm}(\lambda)} \right\} \cdot L(T_{sm}, \lambda) \right] \cdot RSR(B, \lambda) \cdot d\lambda}{RSR(B, \lambda) \cdot d\lambda} \quad (22)$$

In summary  $\overline{L_{EV}(B)}$  is determined by:

$$\overline{L_{EV}(B)} = L_{EV} \left[ a_2^{BCS}(B), a_{SV}^{sm}, a_{EV}^{sm}, a_{BB}^{sm}, a_{cav}(B), a_{BB}(B), T_{BB}(B), RSR(B, \theta), a_0^{BCS}, \overline{b_1^{BB}}, T_{BB}, T_{sm}, T_{CAV}, DN_{EV}, \langle DN_{BB} \rangle, \langle DN_{SV} \rangle \right] \quad (23)$$

where the coefficients

$$a_0^{BCS}(B), a_2^{BCS}(B), a_{SV}^{sm}, a_{EV}^{sm}, a_{OBC}^{sm}, a_{cav}(B), a_{OBC}(B), T_{OBC}(B), RSR(B, \theta)$$

are determined from pre-launch calibration measurements and the remaining coefficients

$$b_1^{BB}, T_{BB}, T_{sm}, T_{CAV}, DB_{EV}, \langle DN_{BB} \rangle, \langle DN_{SV} \rangle$$

are determined from on-orbit telemetry.

### 3.3 On-orbit maneuver for Scan Mirror

The scan mirror for MODIS has a protected-silver coating. This material has the feature that it has different reflectance for s and p polarized light in the infrared striking the mirror away from the mirror normal. These effects also have been documented recently for a similar mirror coating on the GOES imager sensor Weinreb, et. al, 1997. Consequently, in the infrared, the scan mirror has a reflectance which varies with incidence scan angle. We call this response-vs-scan-angle (RVS) behavior.

MODIS has requested that the AM spacecraft be directed to scan deep space for up to about 30 minutes when the spacecraft is in the Earth shadow. This maneuver will provide MODIS a view above the horizon to observe a scene with zero intrinsic incidence infrared radiance onto the scan mirror. With this approach, MODIS will determine the RVS of the scan mirror at all angle of use across the EV aperture. The GOES experience demonstrates further that for the accuracy required of the MODIS measurements, 1 percent or less uncertainty for all emissive infrared bands, that the RVS will change over a year. The GOES imager calibration for RVS is changed quarterly, Weinreb, et. al., 1997! Consequently we are requesting that these cold space scan maneuvers be implemented about yearly.

### 4.0 Reflected Solar-Band Algorithm

The reflected solar bands on MODIS are Bands 1 - 19, and Band 26, covering the wavelength region 0.42 to 2.15  $\mu\text{m}$ . Bands 8 - 19, plus 26 are 1000m bands and have 10 detectors in the track direction. Bands 3 - 7 are 500 m bands and have 20 detectors in the track direction. Bands 1 and 2 are 250 m bands, and have 40 detectors in the track direction. All these detectors are rectangular. Consequently, to fill the individual 1 km field of view in the scan direction, the 500 m detectors are sampled twice, and the 250 m detectors are sampled four times, during the period when the 1000 m detectors are sampled once.

The two primary science data products of the MODIS L1B algorithm, for the reflected solar bands, are the Earth-exiting spectral radiance  $L$ , and the Earth reflectance factor  $\rho \cos(\theta_{sc})$  for each of the 20 bands with a central wavelength between 0.4 and 14.5  $\mu\text{m}$ . Both products are extracted using the effective digital number output,  $dn^*$ .  $dn^*$  are corrected for detector dark radiance response so they could be interpreted as signal. In producing these products, the instrument uses pre-launch calibration factors which can be verified using on-

board calibrators, post launch special tests, vicarious calibrations, ground field tests and lunar observations.

The output from the focal plane detector arrays (FPAs) are digitized, recorded and telemetered as raw digital numbers ( $DN$ ). The instrument response for each band ( $B$ ) and detector channel ( $D$ ) for an individual scene ( $Sc$ ), may be written as:

$$dn_{B,D}^*(Sc) = \left[ DN'_{B,D}(Sc) \cdot S_B(MS, F_{AOI=EV}) - \langle DN'_{B,D}(SV) \rangle \cdot S_B(MS, F_{AOI=SV}) \right] \cdot FF_B(MS, D) \cdot \left\{ 1 + K_{B,D} \left[ \langle T(FP_B) \rangle - T_{Cal}(FP_B) \right] \right\} \quad (23)$$

The non-linearity of the analog to digital converter A/D is used to convert the  $DN$  to  $DN'$ . In this expression,  $S_B(MS, F_{AOI=EV})$  is a lookup table based correction to account for the scan mirror response variation with the mirror angle of incidence (AOI). Each mirror side (MS) is treated separately. The offset correction for the zero radiance response is made using a view of cold space from the solar view (SV) port through the term  $\langle DN'_{B,D}(SV) \rangle$  which is computed from an average of multiple mirror scans. The individual scenes,  $Sc$ , that are used in these bands are scenes in the Earth view, EV, scenes looking at scattering from the solar diffuser, SD, and scenes looking at the SRCA. The AOI reflectance variations in these bands is small.

The correction for temperature variations across the FPA and electronics, as well as the long term temperature variations over the mission lifetime, is applied via a linear correction term which compares the average FP (focal plane) temperature  $\langle T(FP_B) \rangle$  with a reference temperature  $T_{CAL}(FP_B)$ . The temperature coefficient,  $K_{B,D}$ , is determined, for each MODIS detector, based on responsivity variations observed during thermal vacuum testing. The term  $K_{B,D} \left[ \langle T(FP_B) \rangle - T_{Cal}(FP_B) \right]$  is validated on-orbit using a 1W or 10W lamp on with the SRCA over the entire orbit.

Finally,  $FF_B(MS, D)$  is a “flat fielding” calibration term to equalize the response of the individual detectors in a given band based on a post launch observation of a constant scene; at launch time, this correction term is set to unity. On-orbit the  $FF_B$  will be derived from the observations of sunlight scattered off the on-board Spectralon™ Solar Diffuser.

The formulations for the solar reflective bands shown here are based on linear relationships. These formulations are designed with the presumption that the MODIS detectors intrinsically are linear over their operating range for this sensor. Any apparent electronic non-linearity is presumed to be handled explicitly [see Eqn 23)]. The actual situation may not be this way, in which case the actual algorithms coded for the MODIS reflected solar bands products may be somewhat different than are shown here.

The primary calibration for the radiance product is the laboratory SIS-100. The primary calibration for the reflectance factor product is the laboratory measurement of the SD BRF. Measurements of sunlight scattered from the SD, with the SD reflectance stabilized with measurements from the SDSM, provide the primary method to track changes in the calibration for these products through the mission lifetime.

#### 4.1 Radiance Product

The EV band averaged spectral radiance is given by:

$$L_{B,D}(EV) = \frac{\int_{\lambda_1}^{\lambda_2} L_{\lambda}(EV) \cdot R_{\lambda,B,D} d\lambda}{\int_{\lambda_1}^{\lambda_2} R_{\lambda,B,D} d\lambda} \quad (24)$$

where  $L_{\lambda}(EV)$  is the spectral radiance of the Earth scene at wavelength  $\lambda$ ;  $R_{\lambda,B,D}$  is the relative spectral response at wavelength  $\lambda$ , normalized to unity at the peak response;  $\lambda_1$  and  $\lambda_2$  are the wavelength range over which the detector has a significant quantum efficiency.

The pre-launch responsivity is obtained by calibration with a SIS-100 spherical integration source of 100-cm diameter, and is defined by:

$$Cal_{L,B,D} = \frac{dn_{Cal,b,d}(SIS-100)}{L_{Cal,B,D}(SIS-100)} \quad (25)$$

The uncertainty of the calibration of the SIS-100, given in Eqn. 25, by  $L_{Cal,B,D}(SIS-100)$  is validated through EOS Spherical Integration Source comparisons as described in Butler.<sup>1</sup>

The time dependent radiance responsivity,  ${}^*_{L,B,D}(t)$ , is the radiance calibration factor for MODIS at the time,  $t$ . We construct  ${}^*_{L,B,D}(t)$  as a product of the pre-launch value, Eqn 25, the change on transfer to orbit as determined at the first use of the Solar Diffuser (SD), and the change in orbit after the first use of the SD. The current initial operations plans for MODIS will provide measurements with the SD before the Earth View aperture door is opened.

$${}_{L,B,D}(t) = Cal_{L,B,D}(SIS-100) \cdot F_{TTO,B,D} \cdot F(t)_{SD/SDSM,B,D} \quad (26)$$

The transfer-to-orbit factor is preset to unity for all detectors. This quantity is checked on orbit by comparing the response of the MODIS to the SRCA operated in the radiance mode during the ground calibration with the comparable response obtained on-orbit. The radiance product can be checked on-orbit also by comparison of the product

$$Cal_{L,B,D}(SIS-100) \cdot F_{TTO,B,D} \quad (27)$$

with vicarious calibration measurements during the Validation phase of the program, as well as with the reflectance product in conjunction with a standard solar spectral irradiance such as Thullier et. al, 1997. Note that the best use of ground truth-vicarious calibration- in this formulation is to check or correct the calibration scale in Eqn. 27.

$F(t)_{SD/SDSM,B,D}$  is set to unity at launch as well. At the first observations of sunlight scattered off the SD, the SD/SDSM series is initiated. The SDSM is used to correct for changes in the SD scattering function. With the BRDF of the SD corrected by the SDSM data sets,  $F(t)_{SD/SDSM,B,D}$  is re-established for each SD observation sequence at time ( $t$ ),

---

1

smoothed as necessary, and used to “update”  $_{Cal,L,B,D}(t)$  in Eqn. 26. Later in the program, observations of the radiance of sunlight scattered off the moon, observed through the SV port, will be used to validate the  $F(t)_{SD/SDSM,B,D}$  correction term.

Eventually we expect our long-term radiance stability will be fixed with lunar observations, and a term  $F_{Lunar,B,D}(t)$  will replace  $F(t)_{SD/SDSM,B,D}$  in Eqn. 26.

The final calibration expression is:

$$L_{B,D}(EV) = \frac{dn_{B,D}(EV)}{L_{B,D}(t_{EV})} \quad (28)$$

## 4.2 Reflectance Product

In addition to its function as a radiometer, operating in the Earth view radiance mode, MODIS will be used on orbit as a reflectometer. In this mode, MODIS will act as a transfer radiometer between two diffuse reflecting surfaces, the SD and the Earth. The SD and the Earth atmosphere system are reflecting surfaces with a common illuminating source, the sun.

When viewing the Earth, the Earth-atmosphere bi-directional reflectance factor (BRF) is extracted from the EV radiance and the solar irradiance  $E_{SUN,B,D}$  for any detector of a given band by:

$$\rho_{EV,B,D}(t_{SD}) = \frac{\pi L_{B,D}(EV)}{E_{SUN,B,D} \cos(\theta_{EV})} \quad (29)$$

where  $\theta_{EV}$  is the Solar zenith angle on to the scene. A comparison of the Earth BRF to the BRF of the solar diffuser, which is defined in a similar fashion as the above equation, gives the reflectance data product of MODIS, namely:

$$\rho_{EV,B,D}(t_{EV}) \cos(\theta_{EV}) = \frac{L_{B,D}(EV)}{L_{B,D}(SD)} \rho_{SD,B,D}(t_{SD}) \cos(\theta_{SD}) \quad (31)$$

This formulation works well in the instance that the BRF of the SD is flat across the sensor bandpass. For the Spectralon™ diffuser, this is achieved in all the MODIS reflected solar bands, although there is a small error in Band 7 due to the feature at 2.15  $\mu\text{m}$  in the SD,

Guenther, 1997. The ratio of the spectral radiance,  $\frac{L_{B,D}(EV)}{L_{B,D}(SD)}$ , in the above equation

shows the use of MODIS as a ratioing radiometer with the solar diffuser as the reference sample. The above equation can be cast in a form which shows the direct relation to the measured effective digital numbers using the calibration Eqn. 28:

$$\rho(t)_{EV,B,D} \cdot \cos(\theta_{EV}) = \frac{dn_{B,D}(EV)}{dn_{B,D}(SD)} \rho_{SD,B,D}(t_{SD}) \cdot \cos(\theta_{SD}) \quad (32)$$

$$\rho_{SD,B,D}(t_{SD}) = \rho_{SD,Cal,B,D} \cdot F_{TTO,B,D} \cdot F_{SD/SDSM}(t)$$

The SD/SDSM will be used in orbit to track changes in  $\rho_{SD,B,D}$  over time; since the measurement of  $\rho_{SD,B,D}$  is occurring at a different time compared to  $\rho_{EV,B,D}$ , the comparison above also will have to account for differences in the Earth-sun distance. The schedule for repeated solar measurements off the SD will be set so that changes in the

BRF of the SD are small (compared to a 2 percent calibration requirement) between successive observations.

The prelaunch laboratory characterization of the solar diffuser determines its reflectance properties. No system-level calibration of the SD/SDSM will exist. There is no method to monitor changes in this characterization from the laboratory to orbit. The analysis of  $\rho_{SD,B,D}(t_{SD})$  from Eqn. 31 is analogous to that shown for Eqn. 26.

$$\rho_{SD,B,D}(t_{SD}) = \rho_{SD,Cal,B,D} \cdot F_{TTO,B,D} \cdot F_{SD/SDSM}(t) \quad (33)$$

Again,  $F_{TTO,B,D}$  is set to 1, and the term  $\rho_{SD,Cal,B,D} \cdot F_{TTO,B,D}$  can be compared to available ground truth measurements. Eventually we expect our long-term radiance stability will be fixed with lunar observations, and a term  $F_{Lunar,B,D}(t)$  will replace  $F(t)_{SD/SDSM,B,D}$  in Eqn (33).

## 5.0 L1B Data Product Description

The MODIS Level 1B data product contains the radiometrically corrected and fully calibrated instrument data in physical units at the original instrument spatial and temporal resolution.

These data are broken into five-minute granules and stored in Hierarchical Data Format (HDF), separated into the following four files.

**MODIS Level 1B 250M Earth View Data Product** which contains Earth View observations in scientific units for MODIS bands 1 and 2, at 250 meter resolution;

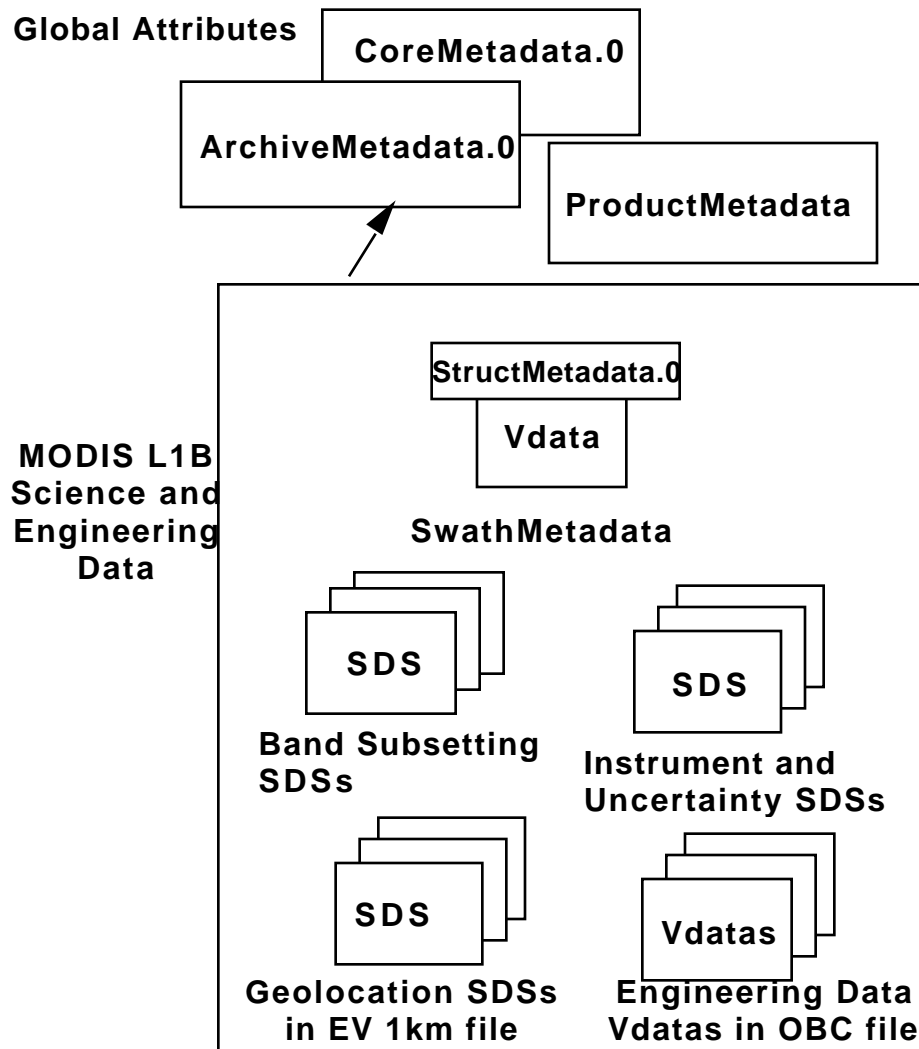
**MODIS Level 1B 500M Earth View Data Product** which contains Earth View observations in scientific units from MODIS bands 1 and 2, aggregated at 500 meter resolution, plus the Earth View observations from MODIS bands 3 through 7, at 500 meter resolution;

**MODIS Level 1B 1KM Earth View Data Product** which contains Earth View observations in scientific units from MODIS bands 1 through 7, aggregated at 1 kilometer resolution, plus the Earth View observations from MODIS bands 8 through 36, at 1 kilometer resolution;

**MODIS Level 1B OBC/E Product** which contains On Board Calibrator observations in scientific units from all MODIS bands, at their original resolution, plus the Engineering data in engineering units.

The aggregation algorithm used in the 500M and 1KM Earth View files is documented in the MODIS Earth Location Algorithm Theoretical Basis document, Version 2.0, April 1995.

The figure below shows the different components of the Level 1B HDF files.



**Level 1B HDF Format**

The product contains five types of metadata which describe the data components, their contents, and their attributes. These are Core Metadata, Archive Metadata, Product Metadata, Swath Metadata, and SDS Metadata. The Core, Archive and Product metadata are stored once in each file as HDF global attributes. The Swath metadata, stored each time data is taken from one scan of one mirror side, is in two forms: swath attributes for HDF-EOS required swath metadata, and HDF Vdata for Level 1B specific swath metadata. The SDS metadata is stored as Scientific Data Set (SDS) attributes and does not explicitly appear in the figure. The various types of metadata are used for different purposes within the production and archive environment. Some is stored in a searchable database for product tracking and queries by science users. The remainder serves as easily accessible descriptive and summary information.

The science data in the Earth View files is instrument data and geolocation data stored as multiple SDSs in HDF-EOS Swath format. External storage of the complete set of geolocation data separated from the swath was approved by ECS for the MODIS project as a means of reducing redundant storage of the geolocation data in every product. The small subset of internal geolocation data stored in the 1 KM Earth View file is for convenience in imaging and visualization. The idiosyncrasies of the way the science data is stored are captured by the self describing capabilities of HDF.

The MODIS instrument observes five scenes or targets from each side of the mirror as the mirror rotates. These targets are the Solar Diffuser (SD), the Spectroradiometric Calibration Assembly (SRCA), the Black Body (BB), the Space View (SV) and the Earth View (EV). The instrument data in three of the four files which comprise the Level 1B or science product are MODIS data taken while observing the EV scene as described above by the algorithms. The instrument data for the four calibration targets viewed by MODIS are stored in the OBC/Engineering file. Both the radiance and reflectance factor products for the reflected solar bands are included in these three science product files.

When the MODIS instrument is commanded to operate in night mode, the data taken from the EV target by the detectors in bands 1 through 19 is not telemetered down from the spacecraft.

The corrected raw counts,  $dn^*$ , from the instrument are stored as 15 bit integers. Meaningful geophysical products for each detector are derived from these integer data by applying the calibration coefficients provided in the attributes.

Invalid data fields are identified by having the high order bit set to 1. The data in a field is marked as invalid for the following reasons:

- it was flagged as missing from the Level 1A dataset;
- the detector is dead;
- the value was saturated;

- there was a calibration failure;
- the radiance was too low to calculate;
- there was coherent Space View (SV) noise;
- the number of outliers in the SV data exceeded the maximum;
- there was a mirror side difference in the SV data.

Thus any data value larger than 32767 should be interpreted as invalid data. The values in data fields that are flagged as missing from the Level 1A dataset are equal to 65535, regarded as unsigned 16 bit integers. For invalid data not flagged as missing from the Level 1A dataset, the actual values stored in the file are the corrected raw counts calculated by the algorithm, stored as 15 bit unsigned integers, with the high order bit of the 16 bit word set to 1.

Associated with each instrument data value is uncertainty information about that value. Uncertainty information is reported as an index. The Uncertainty Index is carried as a multiplicative factor to be applied to the instrument spectral radiance specifications provided below. The uncertainty is recorded as an index which includes MCST's complete and best understanding of the flat-field uncertainties for that pixel. The index translates to an uncertainty value by use of the formula

$$\exp(\text{Uncertainty Index}/2) = \pm \text{Uncertainty Range Multiplier Value.}$$

The uncertainty is carried in the one-sigma sense. This index can be considered a Risk Index describing the use of the Level 1B data. An Uncertainty Index of 7 indicates that the uncertainty has not been computed.

The computation for this index is based on the uncertainty requirement for the typical radiance for each band,  $L_{typ}$ . The sensor specification defines for each band the typical radiance. The specification also allows for an additional uncertainty of 1 percent at any radiance level other than at the  $L_{typ}$  level. As an example, for Band 9, the accuracy requirement of one sigma is 5% for the typical radiance. If the uncertainty index has a value of 3, the maximum magnitude of the range of the uncertainty for Band 9 is  $e^{3/2}(.05)$ , or  $(4.5)(.05) = 0.225$ , or 22.5%.

<b>Uncertainty Index Value</b>	<b>Multiplier Range (1 Sigma)</b>
0	$\pm 1$
1	$\pm 1.6$
2	$\pm 2.7$
3	$\pm 4.5$
4	$\pm 7.4$
5	$\pm 12$
6	$\pm 20$
7	greater than 20,

index not computed

Band	Uncertainty Requirement	Band	Uncertainty Requirement	Band	Uncertainty Requirement
1	5%	13hi	5%	25	1%
2	5%	14lo	5%	26	5%
3	5%	14hi	5%	27	1%
4	5%	15	5%	28	1%
5	5%	16	5%	29	1%
6	5%	17	5%	30	1%
7	5%	18	5%	31	0.50%
8	5%	19	5%	32	0.50%
9	5%	20	0.75%	33	1%
10	5%	21	1%	34	1%
11	5%	22	1%	35	1%
12	5%	23	1%	36	1%
13lo	5%	24	1%		

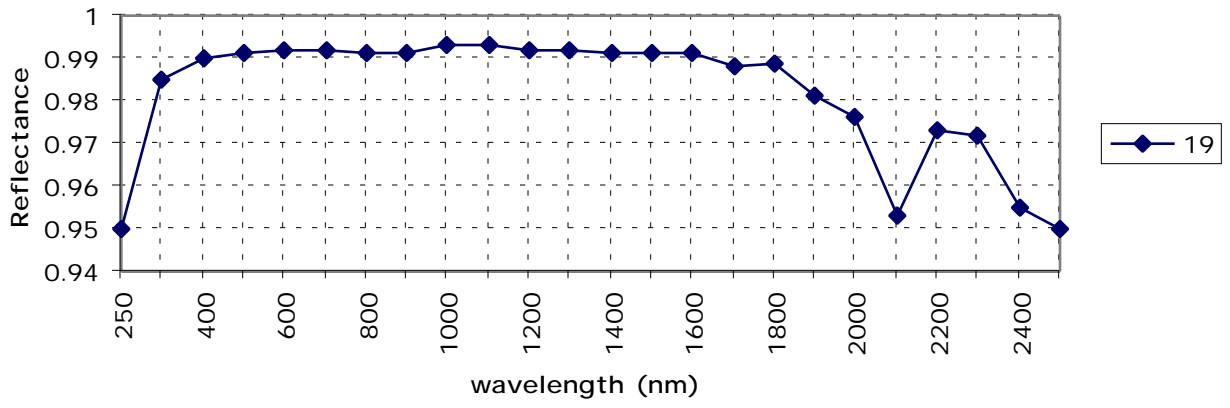
## 6.0 Concluding Comments and Summary

The material describing the at-launch MODIS radiometric product has been presented without a discussion of the actual polarization in the reflected solar bands. The specification for these bands is no greater than 0.02 for bands with a center wavelength between 0.43 and 2.2  $\mu\text{m}$  for Principal Scan Angles between  $+45^\circ$  and  $-45^\circ$ . This performance specification is satisfied for most instances. Nevertheless, variations among detectors in some bands may impact the flat-fielding determination described in Eqn. 23. Data from Bands 1 - 19 are available only when the sensor is operated in the "Day Mode." The operations Day Mode will be performed about 50% of the time of MODIS operations. Band 26 always available.

The formulation of the emissive infrared products are referenced to a radiance scale in this formulation. The Science Team has requested that the products be referenced to brightness temperature, but that correlation is not described here. The published product will be radiance, and added tools from MCST will be provided to obtain brightness temperature from the radiance. The tools will be identified and distributed through the MCST Homepage.

The principle MODIS radiometric products are radiance in the emissive infrared are radiance. The principle MODIS radiometric products in the reflected solar are radiance and reflectance factor. In all three instances an at-launch calibration equation is developed. The techniques to verify the at-launch calibration throughout the mission lifetime are presented. The MODIS data user is instructed to use the MCST Homepage on the World Wide Web for current calibration and characterization parameters.

### Reflectance for Spectralon SRM-990





## 7.0 References

Barnes, William L, Thomas S. Pagano and Vincent V. Salomonson (1998), "Pre-launch performance of the MODerate Resolution Imaging Spectroradiometer (MODIS) on EOS AM-1," IEEE/TGARS.

Esaias, W., "An Overview of MODIS capabilities for ocean science," (1998), IEEE/TGARS.

Guenther, B., (1997) "Ground calibration and in-orbit use of diffusers for Earth observations using MODIS as an example," presented at New Developments and Applications in Optical Radiometry (NEWRAD '97) Tucson, AZ, 27-29 October 1997.

Justice, Christopher, Dorothy Hall, Alfredo Huete, Ranga Myneni, Jan-Peter Muller, Steven Running, Alan Strahler, John Townshend, Eric Vermote and Zhengming Wan (1998) "The MODerate Imaging Spectrometer (MODIS) Mission to Planet Earth enhanced land products description", IEEE/TGARS.

Knowles, D, M. Jones, H. Montgomery, and L.L. Goldberg, (1996) "Algorithm Theoretical Basis Document 1996 Thermal Calibration Algorithm, MCST Reference No. G031.

Labsphere Corporation (1996) "A guide to reflectance materials and coatings," North Sutton, NH 03260.

MacDonald, M (1997), "Testing of mirror reflectance vs. angle of incidence in the PE983 spectrophotometer (draft) Lincoln Laboratory, April 22, 1997.

Masuoka, Edward, Dr. Albert Fleig, Robert Wolfe and Fred Patt (1998), "Key features of MODIS data products and an overview of their production in the EOSDIS," IEEE/TGARS

Thuillier, G., M. Herse, P.C. Simon, D. Labs, H. Mandel and D. Gillotay (1997), "Observations of the solar spectral irradiance from 200 to 850 nm during the ATLAS missions by the SOLSPEC Spectrometer," presented at New Developments and Applications in Optical Radiometry (NEWRAD '97) Tucson, AZ, 27-29 October 1997.

Weinreb, Michael, Michael Jamieson, Nancy Fulton, Yen Chen, Joy Xie Johnson, Carl Smith, James Bremmer and Jeanette Baucom, (1997) "Operational calibration of the imagers and sounders on the GOES-8 and-9 satellites", NOAA Technical Memorandum NESDIS 44, Washington, DC, February 1997.

Young, J, (1997) "PFM MWIR/LWIR radiometric calibration I: theory and measurement equations," SBRS Memorandum PL3095-N06555.